

## Negative Nonlocal Resistance in Mesoscopic Gold Hall Bars: Absence of the Giant Spin Hall Effect

G. Mihajlović,<sup>1,\*</sup> J. E. Pearson,<sup>1</sup> M. A. Garcia,<sup>2</sup> S. D. Bader,<sup>1,3</sup> and A. Hoffmann<sup>1,3</sup>

<sup>1</sup>Materials Science Division, Argonne National Laboratory, Argonne, Illinois 60439, USA

<sup>2</sup>Dpto. Física de Materiales, Universidad Complutense de Madrid, 28040 Madrid, Spain

<sup>3</sup>Center for Nanoscale Materials, Argonne National Laboratory, Argonne, Illinois 60439, USA

(Received 11 February 2009; published 14 October 2009)

We report the observation of negative nonlocal resistances in multiterminal mesoscopic gold Hall bar structures whose characteristic dimensions are larger than the electron mean-free path. Our results can only be partially explained by a classical diffusive model of the nonlocal transport, and are not consistent with a recently proposed model based on spin Hall effects. Instead, our analysis suggests that a quasiballistic transport mechanism is responsible for the observed negative nonlocal resistance. Based on the sensitivity of our measurements and the spin Hall effect model, we find an upper limit for the spin Hall angle in gold of 0.023 at 4.5 K.

DOI: 10.1103/PhysRevLett.103.166601

PACS numbers: 72.25.Ba, 73.23.-b, 85.35.-p

The term nonlocal resistance,  $R_{nl}$ , refers to the generation of a voltage in regions of a multiterminal structure that are outside of the nominal current path. In high mobility, two-dimensional semiconductor heterostructures,  $R_{nl}$  and magnetoresistance (MR) measurements at low temperatures provided valuable insights into understanding electron transport in the ballistic [1,2] and quantum Hall regimes [3]. Such measurements were also applied to study universal conductance fluctuations in diffusive semiconductors and metals in the phase-coherent regime [4], and the flow of vortices in superconducting channels [5]. In hybrid ferromagnet-nonmagnet lateral spin valve structures, nonlocal MR measurements have been utilized to study coherent spin transport phenomena, such as spin diffusion [6,7], spin precession [8], and spin Hall effects (SHEs) [9,10]. Theoretically, it has also been suggested that SHEs should give rise to experimentally observable  $R_{nl}$  in purely paramagnetic structures when the magnitude of the spin Hall angle  $\gamma$ , defined as the ratio of spin Hall and charge conductivities, is sufficiently large [11,12]. However, in this Letter, we present experimental results that show no signatures of such SHE induced  $R_{nl}$  in mesoscopic structures fabricated from gold, which is inconsistent with the recently reported giant  $\gamma$  in this material. We also report the surprising observation of a negative  $R_{nl}$  and show this to be due to a quasiballistic charge transport mechanism not related to SHEs.

Consider a Hall bar structure fabricated from a nonmagnetic normal metal, with two parallel vertical wires of width  $w$  separated by a distance  $L$  and bridged by a horizontal wire of identical width (see Fig. 1), and at temperatures high enough that quantum effects can be neglected. When a current runs through one vertical wire and the voltage is measured across another, a nonzero  $R_{nl}$  appears in the diffusive transport regime when the electron mean-free path  $l_e \ll w$ , because the current density, which spreads into the bridging wire, has a nonzero magnitude in

the region between the voltage probes [see Fig. 1(a)]. The magnitude of this classical  $R_{nl}$ ,  $R_{nl}^c$ , decays exponentially with the distance between the wires at a rate set by the device geometry. Indeed, it follows from the van der Pauw theorem [13] that for  $L \geq w$

$$R_{nl}^c = R_{sq} \exp\left(-\frac{\pi L}{w}\right), \quad (1)$$

where  $R_{sq} = \rho/t$  is the sheet resistance of the wire having resistivity  $\rho$  and thickness  $t$ .  $R_{nl}^c$  is positive, meaning the nonlocal voltage has the same polarity as the one along the direction of current flow in the adjacent wire.

Recently, however, an additional transport mechanism, related to SHEs [14], has been predicted to give rise to nonzero  $R_{nl}$  in a metallic Hall bar structure in the diffusive transport regime [12]. This mechanism is depicted schematically in Fig. 1(b); an electric current flowing through

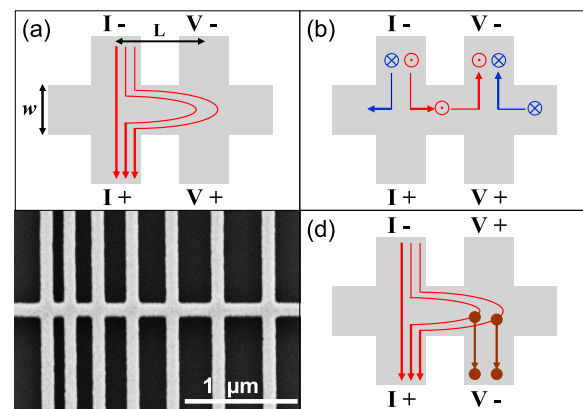


FIG. 1 (color online). Schematic depiction of the physical mechanisms giving rise to (a) positive  $R_{nl}^c$ , (b) positive  $R_{nl}^{SH}$ , and (d) negative  $R_{nl}$  due to quasiballistic transport as described in the text. Arrows indicate the direction of electron flow. (c) SEM image of the central region of the gold Hall bar with seven vertical wires bridged by a horizontal one.

the left vertical wire generates a perpendicular spin current in the bridging wire due to the direct SHE.  $R_{\text{nl}}$  appears because the electrons carrying the spin current scatter preferentially in the same direction (inverse SHE) thus creating a charge accumulation, i.e., voltage across the right vertical wire. Abanin *et al.* calculated [12] that for  $l_e \ll w \ll l_s$ , where  $l_s$  is the electron spin diffusion length, this  $R_{\text{nl}}$  induced by SHEs,  $R_{\text{nl}}^{\text{SH}}$ , can be expressed as

$$R_{\text{nl}}^{\text{SH}} = \frac{1}{2} \gamma^2 R_{\text{sq}} \frac{w}{l_s} \exp\left(-\frac{L}{l_s}\right). \quad (2)$$

$R_{\text{nl}}^{\text{SH}}$  should also be positive (since the potential difference that builds up opposes the electron flow) and, for a given  $L$ , may significantly contribute to  $R_{\text{nl}}$ , if  $l_s$  and  $\gamma$  are sufficiently large. It also follows from Eq. (2) that by analyzing  $R_{\text{nl}}^{\text{SH}}$  as a function of  $L$ , one can simultaneously determine  $l_s$  and  $\gamma$ . Compared to the experiments in which ferromagnets were used to generate or detect spin currents [9,10], this scheme offers an advantage of avoiding complications related to spin injection or detection efficiency of the ferromagnets, which must be known in order to determine  $\gamma$ .

Motivated by these predictions, we fabricated mesoscopic gold Hall bar structures with variable distance  $L$  between adjacent vertical wires and measured  $R_{\text{nl}}$  as a function of  $L$  and temperature  $T$ . Gold was chosen due to its strong spin-orbit coupling, expected to give rise to a large  $\gamma$  value, and at the same time a long enough  $l_s$  value in order to provide a significant value of  $R_{\text{nl}}^{\text{SH}}$  compared to  $R_{\text{nl}}^{\text{c}}$ . Indeed, it has been recently reported that a giant SHE exists in gold, with  $\gamma = 0.113$  at room temperature [10]. Furthermore, values of  $l_s$  of up to 168 nm at 10 K have been reported [15]. Surprisingly, we observed that, in addition to  $R_{\text{nl}}^{\text{c}}$ , the measured  $R_{\text{nl}}$  contains a negative contribution that decays with  $L$  exponentially, as predicted by a classical model, but whose magnitude is also proportional to the fraction of electrons that can travel ballistically over the width of the bridging wire  $w$ , i.e.,  $\propto \exp(-w/l_e)$ . A similar mechanism had been previously observed to give rise to a negative value of  $R_{\text{nl}}$  in structures fabricated from high mobility, two-dimensional electron systems in semiconductor heterostructures, but was typically neglected in nonlocal transport measurements on metallic nanostructures. In addition, based on Eq. (2) and the sensitivity of our measurements, we deduce  $\gamma \leq 0.023$ , which conflicts with the recent observation of a giant SHE in gold.

The Hall bar structures were fabricated on a SiN/Si substrate by  $e$ -beam lithography,  $e$ -beam evaporation, and lift-off. A scanning electron microscopy (SEM) image of the central region is shown in Fig. 1(c). The width and the thickness of the wires were  $w = (110 \pm 4)$  nm and  $t = (60 \pm 2)$  nm, as determined by SEM and atomic force microscopy analysis, respectively. The distance  $L$  between the adjacent vertical wires was varied from 200 to 450 nm in 50 nm steps. All resistance measurements were performed by running an alternating dc current  $I = \pm 0.5$  mA and measuring a dc voltage with a nanovolt-

meter. The resistivity of the polycrystalline gold wires was  $2.07 \mu\Omega \text{ cm}$  and  $3.89 \mu\Omega \text{ cm}$  at 4.5 and 295 K, respectively. These values were negligibly higher ( $\sim 0.04\%$ ) than the ones obtained at a lower current of  $I = \pm 0.1$  mA, which indicates a maximum temperature increase of 5 K at bias currents of 0.5 mA. The corresponding values of  $l_e$ , calculated according to the Drude formula  $l_e = (\hbar/e^2\rho) \times (3\pi^2/n^2)^{1/3}$  were 40.5 and 21.6 nm, respectively, when using an electron density for gold of  $n = 5.9 \times 10^{28} \text{ m}^{-3}$ .

Figure 2 shows the local resistance,  $R = V/I$ , measured between the two vertical wires, separated by 300 nm along the current path (see right inset), from 4.5 to 295 K. In addition to the  $T$  dependence of  $R$ , we also measured the resistance for each segment of the bridging wire between the adjacent vertical wires at 4.5 K. The plot of  $R$  as a function of  $L$  is shown in the inset of Fig. 2. As expected,  $R$  increases linearly with  $L$ . However, the linear fit crosses the  $L$  axis at  $L_0 = (72 \pm 17)$  nm, which indicates that the effective distance between the vertical wires,  $L_{\text{eff}} = L - L_0$ , is shorter than  $L$ . This is most likely caused by spreading of the current density into the voltage leads, due to their finite width.

In contrast to  $R(T)$ , the  $T$  dependence of the nonlocal resistance is unexpected. Figure 3 shows  $R_{\text{nl}}$  vs  $T$  data obtained for  $L = 300$  nm. For other combinations of adjacent vertical wires the data show the same qualitative behavior, but different overall magnitude. At room temperature  $R_{\text{nl}}$  is positive, as expected based on the classical  $R_{\text{nl}}$  mechanism. When  $T$  is lowered  $R_{\text{nl}}$  decreases, but this decrease is not proportional to the decrease of  $R_{\text{sq}}$ , as expected based on Eq. (1). This can be seen in the inset of Fig. 3 where we plot  $R_{\text{nl}}/R_{\text{sq}}$  vs.  $T$ . Based on Eq. (1),  $R_{\text{nl}}/R_{\text{sq}}$  should be a  $T$  independent constant, determined solely by the geometry

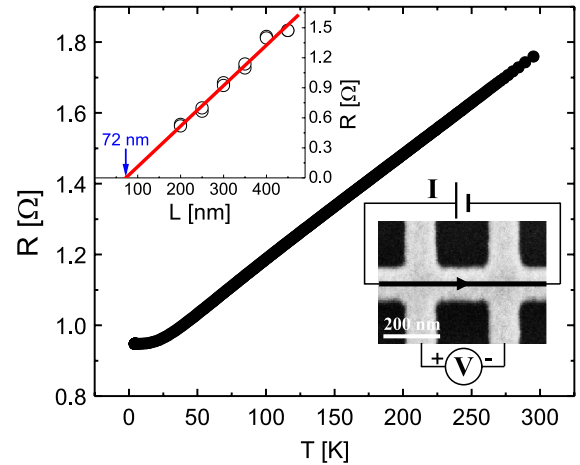


FIG. 2 (color online). Resistance of the bridging wire ( $L = 300$  nm) as a function of  $T$ . Lower inset: SEM image of the segment of the wire whose resistance is plotted, adapted to show the actual measurement configuration. Upper inset: Resistance of each segment of the bridging wire between adjacent vertical wires (open circles) at 4.5 K as a function of  $L$ . The red line is a linear fit to the data.

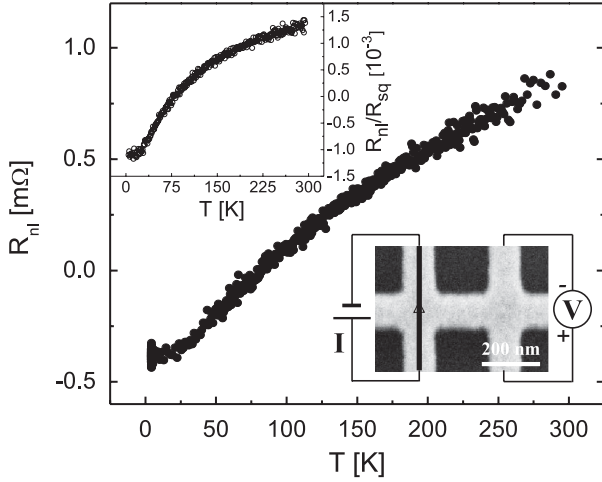


FIG. 3. Temperature dependence of  $R_{nl}$  measured for wires separated by a distance  $L = 300$  nm. Lower inset: SEM image of the segment of the structure where  $R_{nl}$  was measured, adapted to show the actual measurement configuration. Upper inset:  $R_{nl}/R_{sq}$  as a function of temperature.

of the structure. However, we observed that  $R_{nl}/R_{sq}$  is strongly  $T$  dependent. Even more surprisingly,  $R_{nl}$  changes sign with decreasing  $T$ , becoming negative around 82 K, as can be seen in the main plot of Fig. 3. The appearance of the negative  $R_{nl}$  rules out that the SHE mechanism, as suggested in Ref. [12], is responsible for the observed  $T$  dependence of  $R_{nl}/R_{sq}$ .

What transport mechanism could be responsible for the appearance of a  $T$  dependent negative  $R_{nl}$ ? Our bias dependent measurements (not shown) confirmed a linear dependence of the nonlocal voltages on bias current, thus ruling out the possibility that thermoelectric effects arising from Joule heating are responsible for the negative  $R_{nl}$ . On the other hand, previous numerical studies [16] suggest that a negative  $R_{nl}$  can appear due to direct ballistic transmission of electrons into the voltage lead. This purely classical mechanism, however, is expected to be relevant only in structures fabricated from high mobility semiconductor heterostructures where  $l_e$  exceeds characteristic dimensions of the structure. Indeed, negative  $R_{nl}$  has been observed in modulation doped GaAs Hall bar structures in the ballistic transport regime [2]. In order to analyze whether ballistic electrons are responsible for negative  $R_{nl}$  in our structures, we plot  $R_{nl}/R_{sq}$  as a function of  $l_e$ . The plots are shown on Figs. 4(a)–4(f) for all distances  $L$  between the adjacent vertical wires. We find that all the data can be fitted to the formula

$$\frac{R_{nl}}{R_{sq}} = a \left[ 1 - b \exp\left(-\frac{w}{l_e}\right) \right], \quad (3)$$

where  $a$  and  $b$  are dimensionless fitting parameters. Figure 5(a) shows the plot of  $a$  values extracted from the fit as a function of  $L$ . The fitting curve on the graph corresponds to  $a = \exp[-\pi(L - L_0)/w]$  with  $L_0 = (71.1 \pm 0.4)$  nm, in excellent agreement with  $L_0$  obtained from

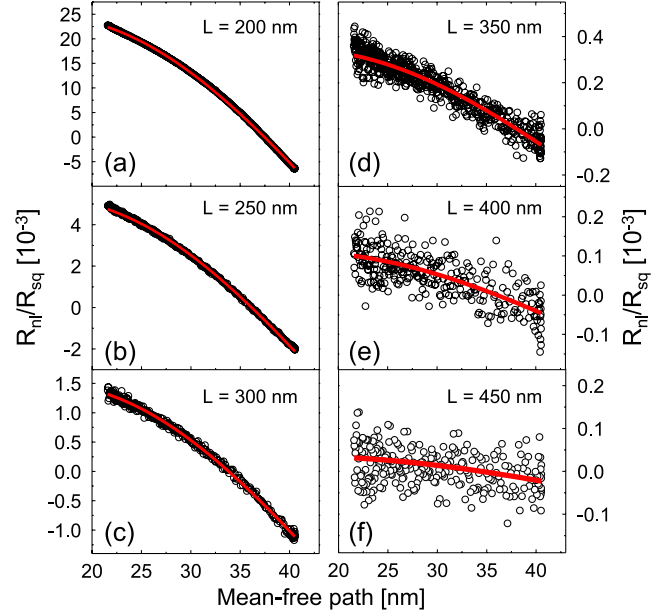


FIG. 4 (color online). (a)–(f)  $R_{nl}/R_{sq}$  as a function of electron mean-free path for different  $L$  values. Corresponding fits to Eq. (3) are shown as red lines.

the local resistance measurements. Therefore, in the completely diffusive limit,  $l_e \rightarrow 0$ , we recover the classically expected  $R_{nl}^c$  with  $L = L_{eff}$  [see Eq. (1)]. In addition, it follows that the negative contribution to  $R_{nl}$ , since it is also proportional to  $\exp(-\pi L_{eff}/w)$ , must originate from the spreading of the current density into the bridging wire. On the other hand, the term  $\exp(-w/l_e)$  in Eq. (3) is the fraction of electrons that can travel ballistically over the distance  $w$ . Thus, we conclude that the negative  $R_{nl}$  comes from electrons that reach the region between the voltage probes diffusively and then, due to their net forward momentum towards the lower voltage lead, they scatter ballistically into it, generating a negative voltage. The proposed mechanism is depicted schematically in Fig. 1(d).

The values of  $b$  extracted from fitting the  $R_{nl}/R_{sq}$  vs.  $l_e$  curves are plotted in Fig. 5(b) for different distances  $L$ .  $b$  varies periodically with  $L$ , which suggests that it is some-

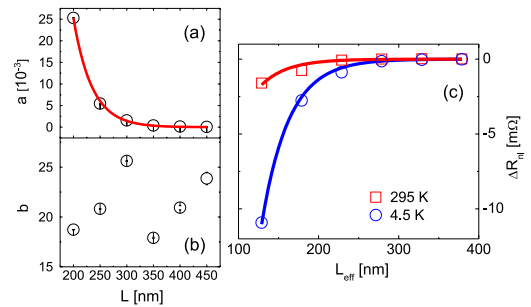


FIG. 5 (color online). (a) Parameter  $a$  vs.  $L$  (open circles) and the best exponential fit (red line) as explained in the text; (b) Parameter  $b$  vs.  $L$ ; (c) Negative  $R_{nl}$  vs.  $L_{eff}$  at 4.5 and 295 K and the corresponding fitting curves explained in the text.



what sensitive to the rebound electron trajectories [16]. The oscillatory behavior of the negative  $R_{nl}$  further supports the explanation that ballistic electrons are responsible for its appearance.

Finally, we subtract  $R_{nl}^c$  from the measured  $R_{nl}$  and plot the data points as a function of  $L_{eff}$  for two different temperatures corresponding to the upper (295 K) and lower (4.5 K) limit of our measurement range. The data were fitted to an exponential function  $\Delta R_{nl} = \alpha \exp(-L_{eff}/\lambda)$  with fixed  $\alpha = -R_{sq}\langle b \rangle \exp(-w/l_e)$ , where  $\langle b \rangle = 21.5$  is the average value of  $b$ , and  $\lambda$  as a fitting parameter. Both data plots and the corresponding fitting curves are shown in Fig. 5(c). We obtain  $\lambda = (33.0 \pm 0.9)$  nm and  $\lambda = (34.0 \pm 0.2)$  nm at 295 and 4.5 K, respectively, both values corresponding to  $w/\pi$ . Therefore, there is no difference in the dependence of the negative  $R_{nl}$  on  $L_{eff}$  at the two limiting temperatures. This further rules out that a transport mechanism related to spin diffusion, as expected for the SHEs, is responsible for the appearance of our negative  $R_{nl}$  values, since it should manifest itself in a  $T$  dependent decay length of the negative  $R_{nl}$ , due to the  $T$  dependence of  $l_s$  [17].

Thus, our experiments do not show the additional positive contribution to  $R_{nl}^c$  expected from SHEs. Using the resolution of our measurements, which is  $20 \mu\Omega$ , and Eq. (2) with  $L = L_{eff} = 128.9$  nm (which corresponds to shortest separation between the vertical wires in our structure) and taking into account the quasiballistic nature of the transport, we can deduce an upper limit for  $\gamma$  of 0.023 at 4.5 K assuming  $l_s = 65$  nm [6], and 0.027 at 295 K assuming  $l_s = 36$  nm. Note that the values of  $\gamma$  in both cases would be even lower if  $l_s$  were longer. Therefore, based on our experiments, the values of  $\gamma$  are at least an order of magnitude lower than the ones reported in Ref. [10]. A possible reason for this discrepancy could be the recent suggestion that Fe impurities and their concomitant Kondo effect could be responsible for a giant  $\gamma$  in gold [18]. To this end, we note that we have not observed an upturn in the resistivity of our structures down to the lowest  $T$ , which would be a signature of such a Kondo effect (see Fig. 2). Another possible reason why a giant SHE was inferred in Ref. [10] could be a strong sensitivity of the nonlocal charge signal to local stray magnetic fields from ferromagnetic components of the structure [19]. It is worthwhile to note that we observe significant  $R_{nl}$  signals, independent of spin transport, in structures with comparable geometries and dimensions as the ones studied in Ref. [10], but their dependence on local magnetic fields is not clear at this point. In general, these effects, that are based only on charge transport, have been neglected in most experiments aimed at nonlocal detection of spin currents.

In conclusion, we report a negative value of  $R_{nl}$  in mesoscopic Hall bar structures fabricated from a nonmagnetic metal, i.e., gold. Our analysis shows that negative  $R_{nl}$  value arises from the effect of ballistic electrons on nonlocal transport, despite the fact that the electronic mean-free paths are smaller than the dimensions of the structure.

In addition, our results do not support the recently reported giant spin Hall effect in gold.

We thank Dimitrie Culcer, Roland Winkler, Oleksandr Mosendz, and Sadamichi Maekawa for useful discussions and comments. This work was supported by DOE BES under Contract No. DE-AC02-06CH11357.

\*mihajlovic@anl.gov

- [1] Y. Takagaki, K. Gamo, S. Namba, S. Takaoka, K. Murase, S. Ishida, K. Ishibashi, and Y. Aoyagi, *Solid State Commun.* **69**, 811 (1989); K. L. Shepard, M. L. Roukes, and B. P. Van der Gaag, *Phys. Rev. Lett.* **68**, 2660 (1992).
- [2] Y. Hirayama, A. D. Wieck, T. Bever, K. von Klitzing, and K. Ploog, *Phys. Rev. B* **46**, 4035 (1992).
- [3] P. L. McEuen, A. Szafer, C. A. Richter, B. W. Alphenaar, J. K. Jain, A. D. Stone, R. G. Wheeler, and R. N. Sacks, *Phys. Rev. Lett.* **64**, 2062 (1990).
- [4] H. Haucke, S. Washburn, A. D. Benoit, C. P. Umbach, and R. A. Webb, *Phys. Rev. B* **41**, 12454 (1990).
- [5] I. V. Grigorieva, A. K. Geim, S. V. Dubonos, K. S. Novoselov, D. Y. Vodolazov, F. M. Peeters, P. H. Kes, and M. Hesselberth, *Phys. Rev. Lett.* **92**, 237001 (2004).
- [6] Y. Ji, A. Hoffmann, J. S. Jiang, and S. D. Bader, *Appl. Phys. Lett.* **85**, 6218 (2004).
- [7] F. J. Jedema, M. S. Nijboer, A. T. Filip, and B. J. van Wees, *Phys. Rev. B* **67**, 085319 (2003); M. Johnson and R. H. Silsbee, *Phys. Rev. Lett.* **55**, 1790 (1985).
- [8] F. J. Jedema, H. B. Heersche, A. T. Filip, J. J. A. Baselmans, and B. J. van Wees, *Nature (London)* **416**, 713 (2002); X. Lou, C. Adelman, S. A. Crooker, E. S. Garlid, J. Zhang, S. M. Reddy, S. D. Flexner, C. J. Palmström, and P. A. Crowell, *Nature Phys.* **3**, 197 (2007).
- [9] S. O. Valenzuela and M. Tinkham, *Nature (London)* **442**, 176 (2006); T. Kimura, Y. Otani, T. Sato, S. Takahashi, and S. Maekawa, *Phys. Rev. Lett.* **98**, 156601 (2007).
- [10] T. Seki, Y. Hasegawa, S. Mitani, S. Takahashi, H. Imamura, S. Maekawa, Y. Nitta, and K. Takanashi, *Nature Mater.* **7**, 125 (2008).
- [11] J. E. Hirsch, *Phys. Rev. Lett.* **83**, 1834 (1999); E. M. Hankiewicz, L. W. Molenkamp, T. Jungwirth, and J. Sinova, *Phys. Rev. B* **70**, 241301(R) (2004).
- [12] D. A. Abanin, A. V. Shytov, L. S. Levitov, and B. I. Halperin, *Phys. Rev. B* **79**, 035304 (2009).
- [13] L. J. van der Pauw, *Philips Tech. Rev.* **20**, 220 (1958).
- [14] M. I. Dyakonov and V. I. Perel, *JETP Lett.* **13**, 467 (1971); M. I. Dyakonov and A. V. Khaetskii, *Spin Hall Effect*, Springer Series in Solid State Sciences Vol. 157 (Springer, New York, 2008).
- [15] J. Ku, J. Chang, H. Kim, and J. Eom, *Appl. Phys. Lett.* **88**, 172510 (2006).
- [16] Y. Takagaki and K. Ploog, *Phys. Rev. B* **49**, 1782 (1994).
- [17] T. Kimura, T. Sato, and Y. Otani, *Phys. Rev. Lett.* **100**, 066602 (2008).
- [18] G. Y. Guo, S. Maekawa, and N. Nagaosa, *Phys. Rev. Lett.* **102**, 036401 (2009).
- [19] F. G. Monzon, H. X. Tang, and M. L. Roukes, *Phys. Rev. Lett.* **84**, 5022 (2000); B. J. van Wees, *Phys. Rev. Lett.* **84**, 5023 (2000).